Dlk1 dosage regulates hippocampal neurogenesis and cognition

Raquel Montalbán-Loro[a,1] , Glenda Lassi[b,c,1] , Anna Lozano-Ureña[a], Ana Perez-Villalba[a,d] , Esteban Jiménez-Villalba[a] , Marika Charalambous[e,2], Giorgio Vallortigara[f] , Alexa E. Horner[g] , Lisa M. Saksida[h,i,j,k], Timothy J. Bussey[h,i,j,k], José Luis Trejo[l] , Valter Tucci[b], Anne C. Ferguson-Smith[e,3], and Sacri R. Ferrón[a,3]

[a]ERI Biotecmed-Departamento de Biología Celular, Universidad de Valencia, 46010 Valencia,Spain; [b]Genetics and Epigenetics of Behaviour (GEB) Laboratory, Istituto Italiano di Tecnologia, 16163 Genova, Italy; [c]Translational Science and Experimental Medicine Research and Early Development, Respiratory and Immunology, BioPharmaceuticals R&D, AstraZeneca, Cambridge Biomedical Campus, Cambridge CB2 0AA, United Kingdom; [d]Faculty of Psychology, Laboratory of Animal Behavior Phenotype (LABP), Universidad Católica de Valencia, 46100 Valencia, Spain; [e]Department of Genetics, University of Cambridge, Cambridge CB2 3EH, United Kingdom; [f]Center for Mind/Brain Sciences, University of Trento, 38068 Rovereto TN, Italy; [g]Synome Ltd, Babraham, Cambridge CB22 3AT, United Kingdom; [h]Department of Psychology, Medical Research Council and Wellcome Trust Behavioural and Clinical Neuroscience Institute, University of Cambridge, Cambridge CB2 3EB, United Kingdom; [i]Molecular Medicine Research Laboratories, Robarts Research Institute, Schulich School of Medicine and Dentistry, Western University, London, ON N6A 5K8, Canada; [j]Department of Physiology and Pharmacology, Schulich School of Medicine and Dentistry, Western University, London, ON N6A 5C1, Canada; [k]The Brain and Mind Institute, Western University, London, ON N6A 5B7, Canada; and [l]Department of Translational Neuroscience, Cajal Institute, The Spanish National Research Council, Madrid 28002, Spain

Neurogenesis in the adult brain gives rise to functional neurons, which integrate into neuronal circuits and modulate neural plasticity. Sustained neurogenesis throughout life occurs in the subgranular zone (SGZ) of the dentate gyrus in the hippocampus and is hypothesized to be involved in behavioral/cognitive processes such as memory and in diseases. Genomic imprinting is of critical importance to brain development and normal behavior, and exemplifies how epigenetic states regulate genome function and gene dosage. While most genes are expressed from both alleles, imprinted genes are usually expressed from either the maternally or the paternally inherited chromosome. Here, we show that in contrast to its canonical imprinting in nonneurogenic regions, *Delta-like homolog 1* (*Dlk1*) is expressed biallelically in the SGZ, and both parental alleles are required for stem cell behavior and normal adult neurogenesis in the hippocampus. To evaluate the effects of maternally, paternally, and biallelically inherited mutations within the *Dlk1* gene in specific behavioral domains, we subjected *Dlk1*-mutant mice to a battery of tests that dissociate and evaluate the effects of *Dlk1* dosage on spatial learning ability and on anxiety traits. Importantly, reduction in *Dlk1* levels triggers specific cognitive abnormalities that affect aspects of discriminating differences in environmental stimuli, emphasizing the importance of selective absence of imprinting in this neurogenic niche.

neurogenesis | genomic imprinting | behavior | gene dosage | hippocampus

Generation of new neurons occurs normally in the adult brain in two locations: the subventricular zone (SVZ) in the walls of the lateral ventricles (1) and the subgranular zone (SGZ) in the dentate gyrus (DG) of the hippocampus (2, 3). Neurogenesis is supported by multipotent neural stem cells (NSCs), astrocytic-like cells that are relatively quiescent and express the stemness-related transcription factor SOX2 (sex determining region Y [SRY]-box 2) (4, 5). In the SGZ, two types of lineage related SOX2+ cells that contribute to neuronal progeny have been identified: the SOX2+ cells with radial processes spanning the granule cell layer and that express the glial fibrillary acidic protein GFAP and Nestin (type one cells) and the nonradial SOX2+ cells (type two) that have short processes, express TBR2, and arise from the radial population (6, 7). Radial SOX2+ cells are the source of stem cells in the DG and rarely divide, whereas nonradial cells cycle more often, being suggested as the intermediate precursor (8). Both the horizontal and radial progenitors respond differently to neurogenic stimuli, suggesting that in the SGZ, there are different populations of progenitors with different properties (9). Type two cells generate in turn type three cells, which are neuronal precursors that express

markers of immature migrating neurons, such as doublecortin (DCX) and the polysialylated neural cell adhesion molecule (PSA-NCAM). Once formed, new neurons migrate to the granule cell layer (GCL) of the DG, where they develop morphological and functional properties of granule neurons and integrate neuronal circuits into the hippocampal CA3 region, forming dendrites and spreading their axons, modifying the existing circuitry (7, 10). In addition to the production of granular neurons, a low percentage of activated NSCs divide asymmetrically to give rise to astrocytes. The latter migrate into the hilus and the molecular layer, where they lose their stem cell potential (11). Hippocampal NSCs can be isolated from the DG and cultured in vitro in the presence of the epidermal growth factor (EGF) and basic fibroblast growth factor (bFGF) mitogens, forming

Significance

Generation of new neurons occurs normally in the adult brain in two locations: the subventricular zone (SVZ) in the walls of the lateral ventricles and the subgranular zone (SGZ) in the dentate gyrus (DG) of the hippocampus. Neurogenesis in the adult hippocampus has been implicated in cognitive functions such as learning, memory, and recovery of stress response. Imprinted genes are highly prevalent in the brain and have adult and developmental important functions. Genetic deletion of the imprinted gene *Dlk1* from either parental allele shows that DLK1 is a key mediator of quiescence in adult hippocampal NSCs. Additionally, *Dlk1* is exquisitely dosage sensitive in the brain with perturbations in levels resulting in impaired NSCs function and cognitive phenotypes.

free-floating aggregates called "neurospheres" (12, 13). Self-renewal and multipotency characteristics of NSCs are assessed in vitro by clonal analysis in which single cells give rise to neurospheres (14, 15).

Neurogenesis in the adult hippocampus has been implicated in cognitive functions such as learning, memory, and recovery of stress response (16–19) as well as contributing significantly to hippocampal plasticity throughout the life span (20, 21). However, how adult neurogenesis contributes to hippocampal function is largely unknown. The hippocampus is involved in memory formation as well as spatial navigation. Indeed, promotion or suppression of hippocampal neurogenesis corresponds with improvement or impairment in learning and memory performance, respectively (17, 18, 22, 23). Both specific brain circuits within the hippocampus and adult neurogenesis, have been suggested as modulatory mechanisms for the encoding of spatial/contextual information (23, 24). Notably, the discrimination between memorized similar stimuli (e.g., a particular location) and the new stimulus conditions (e.g., a new location) are fundamental sensory/cognitive mechanisms that pave the way for the reorganization of complex behaviors and cognitive processes. Importantly, these processes are shared across many species, including mice and humans (25). A functional role for hippocampus neurogenesis in spatial pattern separation has also been demonstrated with lesions of the DG circuitry, resulting in impaired pattern separation-dependent memory (17, 26, 27). Furthermore, an excessive pattern separation prevents the integration of multiple information within the environment and results in cognitive inflexibility, anxiety, and excessive attention to details as manifested in autism and obsessive-compulsive disorders (23). Thus, adult neurogenesis in the hippocampus serves as a normal cellular process for learning and memory consolidation.

Genomic imprinting is an epigenetic process that causes genes to be expressed according to their parental origin, resulting in activation of one of the two alleles of a gene and repression of the other (28). Imprinted genes are highly prevalent in the brain and have adult and developmental important functions (29, 30). The vertebrate-specific atypical NOTCH ligand Delta-like homolog 1 (*Dlk1*) is an imprinted gene that encodes membrane-bound and secreted isoforms that function in several developmental processes (31–34). We have previously shown that mice deficient in *Dlk1* have defects in postnatal SVZ neurogenesis, resulting in depletion of mature neurons reaching the olfactory bulb. DLK1 is secreted by SVZ niche astrocytes, whereas its membrane-bound isoform is present in NSCs and is required for the inductive effect of secreted DLK1 on self-renewal within this niche (33). In most human and mouse tissues, *Dlk1* is expressed only from the paternally inherited chromosome (35, 36). However, in the SVZ, there is a requirement for *Dlk1* to be expressed from both maternally and paternally inherited chromosomes (33), suggesting that modulation of imprinting might be specific in different developmental contexts. Nothing is known about the imprinting status of *Dlk1* in the adult SGZ and its role in adult hippocampal function. Although most of the work on imprinted genes has centered on fetal and early postnatal growth, growing evidence suggests that many imprinted genes also influence cognition and a wide range of behaviors (37–41). Indeed, the role of imprinted genes in synaptic function and plasticity suggests a pivotal role in learning and memory (30). For instance, deficiencies in contextual memory are observed when *Ube3a*, *Ppp1r9a*, or *Rasgrf1* are absent (42–44), and *Igf2* has been shown to be necessary for memory consolidation (45). Here, we test the requirement of DLK1 signaling for the regulation of DG NSCs and evaluate the effects of maternal and paternal heterozygous mutations and homozygous mutations of the *Dlk1* gene in specific behavioral and cognitive domains that involve hippocampus circuits.

Genetic deletion of *Dlk1* from either parental allele shows that DLK1 is a key mediator of quiescence in adult hippocampal NSCs. Additionally, we have subjected *Dlk1*-deficient mice to spatial learning tasks (geometry test), anxiety-like assessments (elevated plus maze), and discrimination tests (touch screen task). Within this battery of behavioral tests, we dissociated the effects of *Dlk1* dosage on learning ability, on pattern separation and completion, and on repetitive/anxiety traits. Taken together, our evidence indicates that *Dlk1* is exquisitely dosage sensitive in the brain, with perturbations in levels resulting in impaired NSCs function and cognitive/psychiatric phenotypes.

Results

Biallelic Expression of *Dlk1* Is Required for Adult Hippocampal Neurogenesis. Previous studies have suggested that radial glia-like cells, which express GFAP and Nestin and form neurospheres in vitro, are NSCs in the hippocampal SGZ (13, 46). We first examined *Dlk1* expression in the DG of the adult mouse hippocampus using qPCR and immunohistochemical analysis. We observed that *Dlk1* is present in NSCs derived from the adult SGZ and in double GFAP/SOX2+ cells in the wild-type hippocampus in vivo (Fig. 1 *A* and *B*), but on the contrary to the SVZ, differentiated astrocytes from the SGZ show very low levels of expression of this gene (Fig. 1*A*). Alternatively, spliced transcripts of *Dlk1*-encoding protein isoforms that are either membrane tethered or proteolytically cleaved and secreted have been described (33, 47). In the adult hippocampus, we found that both the *Dlk1* membrane bound and the secreted isoforms are expressed (*SI Appendix*, Fig. S1A). However, the secreted isoform represents the predominant type in the SGZ NSCs (*SI Appendix*, Fig. S1A), also contrary to what it happens in the SVZ NSCs (33), suggesting a different mechanism of action of *Dlk1* in this neurogenic niche.

Dlk1 is canonically expressed from the paternally inherited chromosome (35, 48); thus, to study whether the imprinting state of the gene is maintained in the adult hippocampus, we next examined *Dlk1* expression from each of the two parental chromosomes. To do so, we determined *Dlk1* allele-specific activity in the SGZ of wild-type F1 hybrid offspring from reciprocal crosses of *Mus musculus domesticus* (C57BL6/J) and *Mus musculus castaneus* (CAST/EiJ) strains, in which a single-nucleotide polymorphism (SNP) was identified between the two subspecies at the *Dlk1* gene (*SI Appendix*, Fig. S1B). Whereas whole hippocampus tissue from reciprocal hybrids showed the expected paternally inherited imprinted expression of *Dlk1*, the adult NSCs showed biallelic (nonimprinted) expression of the gene (Fig. 1*C*) as was previously shown in NSCs derived from the SVZ (33). Importantly, other imprinted genes, such as the adjacent *Gtl2* (also known as *Meg3*) and *Snrpn* genes, maintained their imprinting state in SGZ NSCs (Fig. 1*C* and *SI Appendix*, Fig. S1 *B* and *C*) and did not alter their expression levels (*SI Appendix*, Fig. S1F). This identifies a previously undescribed biallelic expression of specifically *Dlk1* in the adult hippocampus neurogenic niche.

In order to investigate the role of *Dlk1* in DG neurogenesis in vivo, we analyzed the SGZ of wild-type, maternal (*Dlk1^{mat/+}*), or paternal (*Dlk1^{+/pat}*) heterozygotes and of *Dlk1* homozygous (*Dlk1^{−/−}*) mice (33) for *Dlk1* mutation. We first demonstrated by qPCR and immunocytochemical analysis that *Dlk1* was reduced in NSCs derived from the SGZ of *Dlk1^{mat/+}* or *Dlk1^{+/pat}* heterozygotes (Fig. 1D and *SI Appendix*, Fig. S1 *D* and *E*), confirming absence of imprinting in this niche. To assess any functional relevance of this and the possibility that *Dlk1* can regulate proliferation of NSCs in the SGZ, as we had previously described for the SVZ (33), 2-mo-old *Dlk1* mutant mice were injected with the nucleotide analog BrdU 3 wk prior to killing (Fig. 2*A*). Based on proliferation capacities, two major classes of cells are expected to retain the BrdU label in the DG of the hippocampus: slowly dividing SOX2+ NSCs that do not dilute the BrdU through division (named as label retaining cells, LRC-BrdU) and newborn neurons that incorporate BrdU prior to cell
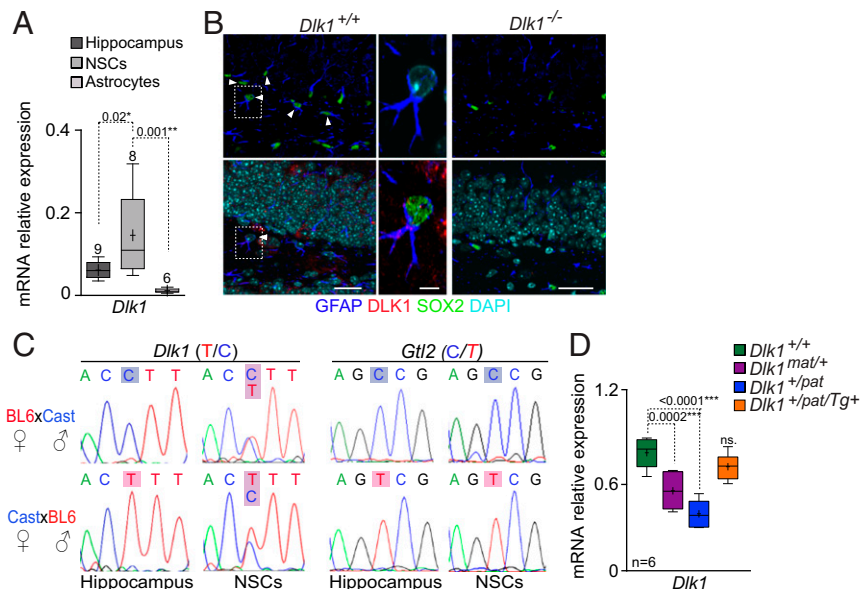
Fig. 1. *Dlk1* is biallelically expressed in the SGZ NSCs and astrocytes. (*A*) qPCR of *Dlk1* expression in hippocampus tissue and in NSCs and differentiated astrocytes derived from the SGZ of wild-type mice. (*B*) Immunohistochemistry for GFAP (blue), SOX2 (green), and DLK1 (red) within the SGZ of the hippocampus of wild-type and *Dlk1*-null mice. High magnification images of triple positive cells are shown. DAPI was used to counterstain nuclei. (*C*) *Dlk1* and *Gtl2* allele-specific expression in hippocampus tissue and NSCs cDNAs obtained from reciprocal F1 offspring of *Mus musculus domesticus* C57BL/6 (BL6) and *Mus musculus castaneous* CAST/EiJ (Cast) strains. SNP position is indicated. (*D*) qPCR of *Dlk1* expression in SGZ tissue of wild type (*Dlk1$^{+/+}$*), heterozygotes upon maternal (*Dlk1$^{mat/+}$*), or paternal (*Dlk1$^{+/pat}$*) transmission of the mutation. Paternal transmission *Dlk1* mutants that were hemizygous for a *Dlk1*-expressing transgene (*Dlk1$^{+/pat}$;Dlk1$^{tg/+}$*) were also analyzed. Data are expressed relative to *Gapdh*. *Dlk1$^{-/-}$* NSCs show no expression of the gene. All error bars show SEM. One-way ANOVA and Tukey's or Dunnett's posttest were used. *P* values and number of samples are indicated. ns., nonsignificant. (Scale bars in *B*: 20 μm; high magnification: 7 μm.)

cycle exit (*SI Appendix*, Fig. S2*A*). Among the cells that retained BrdU, we quantified the proportion of GFAP/SOX2+ undifferentiated cells in *Dlk1* mutant mice and observed that the total number of SOX2+ cells was diminished through a reduction in both SOX2+ radial and nonradial cells (Fig. 2 *A–D*). Additionally, as measured by anti-Ki67, GFAP/SOX2+ proliferation was diminished, indicating a restriction in the proliferative activity in the SGZ in both maternal and paternal *Dlk1* heterozygous mice (Fig. 2 *C* and *D*). We next counted neuronal progenitors and immature neurons, identified by their positivity for TBR2 and DCX, respectively, and observed significantly less TBR2+ progenitor cells in *Dlk1* mutant mice (*SI Appendix*, Fig. S2 *B–D*). *Dlk1* deletion also resulted in significantly less DCX+ immature neurons compared with controls (Fig. 2 *E* and *F*), although their proliferation activities were not affected (*SI Appendix*, Fig. S2*C*). As a result, the number of BrdU+-LRC/ NeuN+ differentiated progeny was significantly reduced in the granular layer of the SGZ after both maternal and paternal transmission of the mutation (Fig. 2*F*). Importantly, *Dlk1* homozygous mutants showed a more severe reduction in the number of undifferentiated GFAP/SOX2+ and newborn cells in the SGZ, suggesting a dosage-dependent effect of the protein (Fig. 2 *B*, *D*, and *F*). We confirmed that these phenotypes were specifically due to a reduction in the available levels of DLK1 by generating paternal transmission *Dlk1* mutants that were also hemizygous for a *Dlk1*-expressing transgene (*Dlk1$^{+/pat}$/Tg+*) (Fig. 2*B*). The number of GFAP/SOX2/BrdU-LRCs and GFAP/ SOX2/Ki67 cells in the transgene-containing mutant SGZ tissue was not significantly different from that obtained in wild-type littermates, indicating that rescue of the mutation by the intact transgene had occurred in vivo (Fig. 2 *B* and *D*). Interestingly, overexpression of *Dlk1* in the brain did not have an effect on the distribution of the different cell populations in the intact SGZ, as indicated by the proportion of GFAP/SOX2 positive cells in the DG of *Dlk1* transgenic mice (48) (*SI Appendix*, Fig. S3 *A–C*).

These results demonstrated that *Dlk1* regulates hippocampal neurogenesis in young mice and that selective absence of imprinting and therefore biallelic expression of the gene in the NSCs in the DG is required for the maintenance of stem cells in the SGZ neurogenic niche.

Dlk1 Regulates Self-Renewal of Postnatal NSCs in the SGZ. To investigate the specific role of *Dlk1* on the self-renewal capacity of neural progenitors, we assessed whether the same phenotype could be reproduced in vitro under experimentally controlled conditions. In support of the in vivo data, the number of primary neurospheres isolated from the DG at different postnatal ages was reduced in *Dlk1*-deficient mice compared to controls (Fig. 3*A* and *SI Appendix*, Fig. S4 *A* and *B*). Again, *Dlk1* homozygous mutant cultures showed a more severe reduction in the number of primary spheres than heterozygote, suggesting a dosage-dependent effect of the protein also in vitro (Fig. 3*A* and *SI Appendix*, Fig. S4 *A* and *B*). Consistently, no effects on the proportion of primary neurospheres obtained from the SGZ were observed in *Dlk1*-transgenic mice overexpressing *Dlk1* (*SI Appendix*, Fig. S3*D*). It has been demonstrated that disruption of quiescence leads to loss of stem cell potential and depletion of the NSC pool with age (16, 49). To test whether DLK1 was required for NSC maintenance in the aged SGZ, we determined the yield of primary neurospheres from 2-, 5-, 8-, and 12-mo-old mutant DG. Aged *Dlk1*-deficient mice showed a more severe progressive decline in the number of primary neurospheres than wild-type mice from the same age (Fig. 3*A*). Moreover, this decline was more acute in *Dlk1$^{-/-}$* than in heterozygote cultures, confirming that a *Dlk1* dose is important for NSC behavior in the SGZ (Fig. 3 *B–E*). The number of in vitro neurospheres obtained from *Dlk1$^{+/pat}$/Dlk1Tg* double-mutant SGZ tissue was not significantly different from the number obtained from wild-type littermates (Fig. 3*A*), indicating that rescue of the mutant had
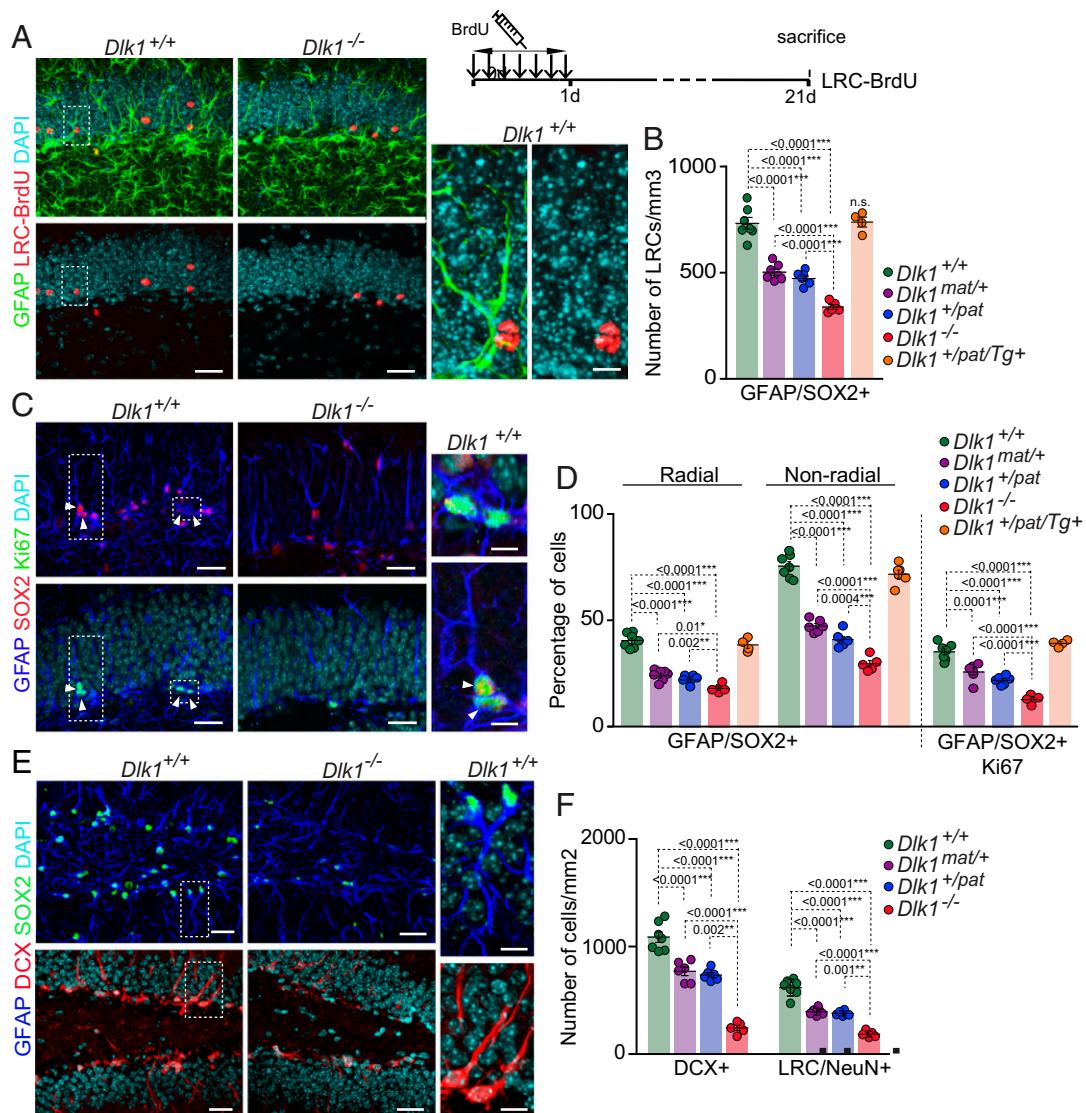
Fig. 2. *Dlk1* regulates adult hippocampal neurogenesis. (*A*) Schematic drawing of the BrdU injection protocol. Immunohistochemistry for GFAP (green) and BrdU-LRCs (red) within the SGZ of the hippocampus in *Dlk1*$^{+/+}$ and *Dlk1*$^{-/-}$ mice (*Left*). High magnification images are shown (*Right*). (*B*) Quantification of the total number of LRC-BrdU that are double positive for GFAP and SOX2. (*C*) Immunohistochemistry for GFAP (blue), SOX2 (red), and Ki67 (green) within the SGZ of the hippocampus in *Dlk1*$^{+/+}$ and *Dlk1*$^{-/-}$ mice. High magnification images are shown (*Right*). (*D*) Quantification of the percentage of GFAP radial and nonradial cells that are positive for SOX2 in the SGZ of the different genotypes. Percentage of GFAP/SOX2 cells that are also positive for the proliferation marker Ki67 is included. (*E*) Immunohistochemistry for GFAP (blue), DCX (red), and SOX2 (green) within the SGZ of the hippocampus in *Dlk1*$^{+/+}$ and *Dlk1*$^{-/-}$ mice. High magnification images are shown (*Right*). (*F*) Quantification of the total number of DCX+ cells and newborn LRC-NeuN+ neurons in the SGZ of the hippocampus of *Dlk1* mutant mice. DAPI was used to counterstain nuclei. All error bars show SEM. One-way ANOVA and Sidak multiple comparison tests were used. *P* values and number of samples are indicated. (Scale bars in *A*, *C*, and *E*: 30 μm; high magnification images: 7 μm.)

occurred also in vitro and that accelerated exhaustion of the stem cell pool was due to a reduction of DLK1 levels.

To next characterize the self-renewal capability of *Dlk1*-deficient cultures, primary neurospheres were individually dissociated into single cells and plated at clonal density (2.5 cells/μl) (*SI Appendix*, Fig. S4A). *Dlk1*-deficient NSCs exhibited a significant reduction in the number of secondary neurospheres formed at early passages (Fig. 3B). To determine whether this reduction in the self-renewal capacity defect in *Dlk1* deficient cultures could be due to a proliferation or survival defect, we performed a tetrazolium salt (MTS) colorimetric assay, which showed a reduction in the proportion of metabolically active cells in the neurosphere cultures of both maternal and paternal *Dlk1* heterozygous SGZ (Fig. 3C). Accordingly, cell cycle analysis by flow cytometry indicated that *Dlk1* mutation reduced the proportion of

hippocampal NSCs in S-phase (Fig. 3D). This decrease in proliferation was not due to cell death given that the propidium iodide labeled cells were 1.45% ± 0.85% in wild-type cultures versus 1.78% ± 0.64% in *Dlk1* mutant cultures. Furthermore, multipotentiality in clonal differentiation assays was decreased in *Dlk1*-deficient NSCs as indicated by the percentage of clones with the capacity to give rise to the three types of cells from the central nervous system (astrocytes, oligodendrocytes, and neurons) (Fig. 3E). Therefore, the compromised self-renewal and multipotency capacities in *Dlk1*-deficient NSCs is caused by an effect on the overall proliferation rate and differentiation efficiency upon both maternal or paternal transmission of the mutation. It is worth noting that, in contrast to the SVZ, in which DLK1 acts as a niche-secreted factor (33), NSCs in the SGZ do not respond to exogenously added DLK1 (Fig. 3B).
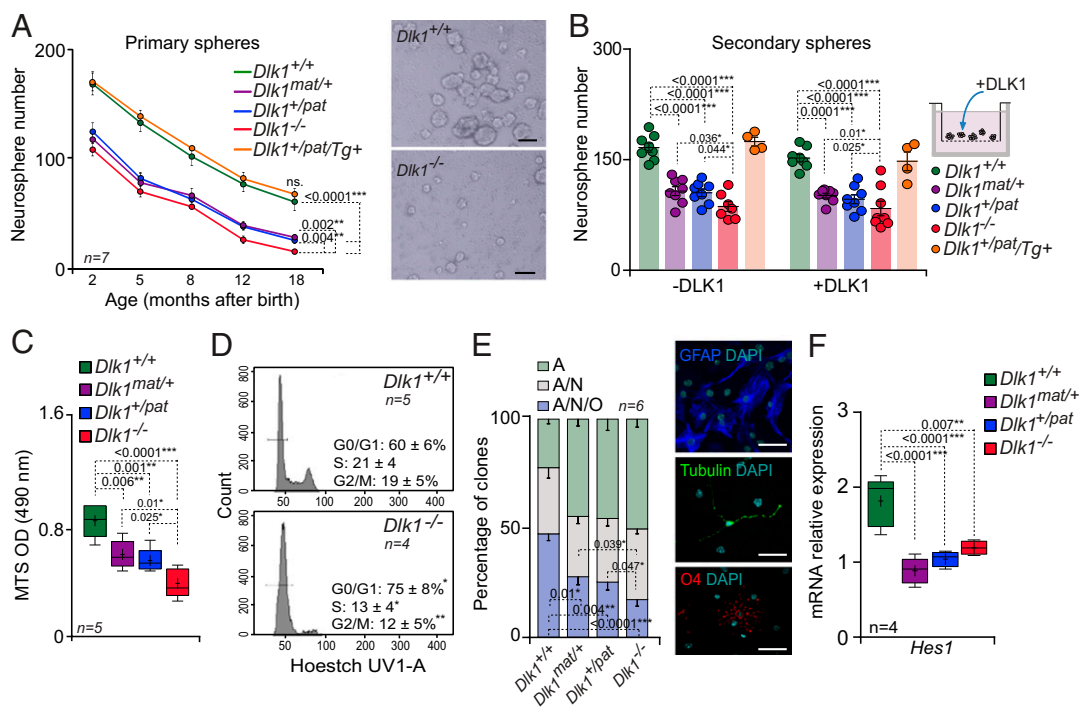
Fig. 3. Absence of *Dlk1* leads to the exhaustion of the NSCs pool in the adult SGZ. (*A*) Number of primary spheres in wild type, *Dlk1$^{mat/+}$*, *Dlk1$^{+/pat}$*, and *Dlk1*-mutant SGZ at different postnatal stages showing a reduction of the number of neurospheres, which is accelerated in the aged *Dlk1* mutant mice (*Left*). Neurospheres from *Dlk1$^{+/pat}$;Dlk1$^{tg/+}$* mice were also analyzed. Representative images of the primary neurosphere cultures obtained from wild type and *Dlk1* mutant SGZ (*Right*). (*B*) Quantification of the number of secondary neurospheres formed after 6 d in vitro in *Dlk1$^{+/+}$* and *Dlk1*-deficient NSC cultures treated or not with recombinant DLK1. (*C*) MTS colorimetric quantification of viable cells in proliferating NSC-SGZ cultures. (*D*) Cell cycle analysis of neurosphere cultures expanded from the SGZ in wild type and *Dlk1$^{-/-}$*, showing a reduced proliferation capacity in the mutant cultures. (*E*) Quantification of unipotent (astrocytes, A), bipotent (astrocytes/neurons, A/N), and tripotent (astrocytes/neurons/oligodendrocytes, A/N/O) clones derived from wild type and *Dlk1* mutant NSC cultures (*Left*). Immunocytochemistry for the astrocyte marker GFAP (blue), the neuroblast marker βIII-tubulin (green), and the oligodendrocyte marker O4 (red) in differentiated neurospheres (*Right*). (*F*) qPCR of *Hes1* expression in NSCs derived from *Dlk1$^{+/+}$*, *Dlk1$^{mat/+}$*, *Dlk1$^{+/pat}$*, and *Dlk1$^{-/-}$*. All error bars show SEM. Simple linear regression was applied in *A*. One-way ANOVA and Sidak multiple comparison tests were used in *B*, *C*, *E*, and *F*. Unpaired *t* tests were performed in *D*. *P* values and number of samples are indicated. ns., nonsignificant. (Scale bars in *A*: 100 μm; in *E*: 20 μm.)

Moreover, a change in the levels of the NOTCH effector *Hes1* was observed in *Dlk1*-deficient NSCs (Fig. 3*F*), suggesting that DLK1 acts in an autocrine manner in the adult DG.

Full Absence of *Dlk1* Correlates with Anxiety-Like Phenotypes. We next examined the differences in behavior of the *Dlk1*-deficient mice in the elevated plus maze (EPM). This test is used to measure anxiety-related traits based on the innate aversion of rodents to open areas and on the spontaneous exploratory behavior of the animals (Fig. 4*A*). It is considered that the time spent in the open arms of the maze is inversely correlated to their level of anxiety (50). The overall activity was estimated by the total distance traveled during a 10-min observation period, and interestingly, this parameter was not affected in *Dlk1*-deficient mice, indicating no change in overall ambulatory behavior (*SI Appendix*, Fig. S5*A*). However, *Dlk1$^{-/-}$* mice spent less time in open arms as compared to wild-type mice (Fig. 4*B*). Also, the number of entries in open arms was reduced in homozygous mice (Fig. 4*B*). Interestingly, *Dlk1* heterozygous mice, *Dlk1$^{mat/+}$* or *Dlk1$^{+/pat}$*, did not show any change in time spent or entries (Fig. 4*B*). Moreover, the frequency of defecations (fecal boli) and urination (urine patches) shed was significantly increased only in homozygous mutant mice relative to the wild-type or heterozygous animals (*SI Appendix*, Fig. S5*B*), consistent with defective autonomic responses in anxiogenic contexts. These findings indicate that complete absence of *Dlk1* results in anxiety-like behaviors.

Maternal and Paternal Expression of *Dlk1* Regulates Spatial Navigation. Adult hippocampus neurogenesis is considered to be involved in cognitive functions that are essential for humans

(20). For example, spatial navigation has been traditionally ascribed to the functions of the hippocampus. However, in traditional assessments of spatial navigation in rodents, it is difficult to test whether the animal is capable of deriving spatial information from boundary-based "geometry" features or from landmarks (51). Both geometry-like and landmark spatial references are essential properties of the environment, and their use during correct navigation is advantageous, as testified in many species (45, 51, 52). Moreover, the ability to derive spatial references from reduced landmark information allows the capture of spatial learning independently from performance or reinforcement (53).

In an effort to investigate the precise role of maternal and paternal expression of *Dlk1* in the regulation of spatial navigation, we used a spatial test in which we compared the spatial ability of mice to navigate across a water tank either in a condition with clear landmarks or in a condition in which the main visible landmarks were reduced. In the latter condition, the animal must rely more on the environmental surface of the tank (52, 54). *Dlk1* heterozygotes and homozygous 2-mo-old mutant mice were tested. The assay consisted of a white rectangular tank filled with water mixed with nontoxic white paint to ensure the invisibility of a platform (Fig. 4*C*). The platform was maintained just below water level and kept during the training phase of the test. Each trial started when the animal was introduced to the tank and lasted until the mouse reached the platform. All animals explored the arena to find the platform. The rationale of this test was to assess the capability of the mice to acquire spatial information from a visible landmark or from prevalently boundary
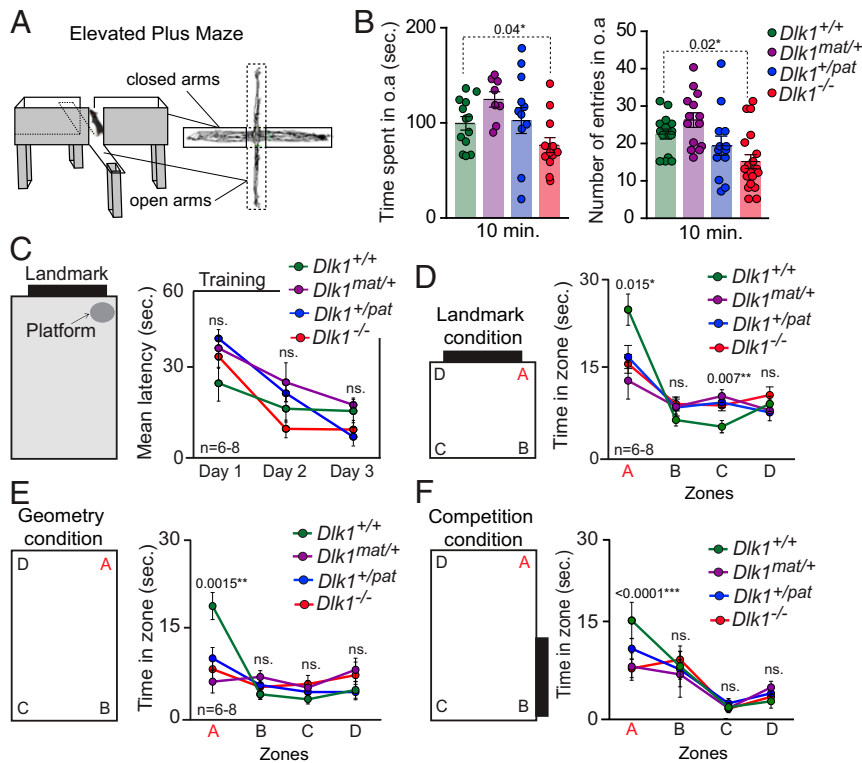
Fig. 4. Maternal and paternal expression of *Dlk1* controls spatial navigation. (*A*) Schematic drawing of the EPM system. (*B*) Time spent and number of entries in open arms by the different animals after a 10-min observation period. *Dlk1*$^{-/-}$ mice showed fewer number of entries and less time spent in open arms than their wild-type littermates. (*C*) Schematic representation of the tank, landmark, and platform used for the geometric test. The test is performed in a white rectangular tank, convertible in a square, with a platform and a black landmark (*Left*). Mean latency in the training phase (day 1 to day 3; *Right*). (*D*) Schematic representation of the landmark condition. The tank is a square with no platform. A, B, C, and D indicate the four zones in the tank. The time spent in each zone was monitored and represented for each group of mice (*Right*). (*E*) Schematic representation of the geometry condition with no landmark or platform (*Left*). The time in each zone is represented in the graph (*Right*). Wild-type animals spent significantly more time in the zone "A" where the platform was located both in landmark and geometry conditions. (*F*) Schematic representation of the competition condition with a rectangular tank and the landmark located in a different zone (*Left*). The time in each zone is represented again in the graph (*Right*). All error bars show SEM of at least eight animals per genotype. One-way ANOVA and Sidak multiple comparison tests were used. Two-way ANOVA was applied in *C–F*. P values and number of samples are indicated. ns., nonsignificant.

information in which the visible landmarks were removed. The training was spread across 3 consecutive days with daily sessions of three trials. After training, we subjected all animals to a series of probe trials in which the platform was removed, and the spatial navigation of the animals was monitored and analyzed. Within the tank, a black landmark was positioned on the short wall above the platform and stayed there for the whole training (Fig. 4*C*). When testing, in the "Landmark" condition, the tank was converted into a square arena with the landmark located on the same wall as in the training condition (Fig. 4*D*). For the "Geometry" condition, the tank was maintained in its rectangular shape with no visible landmark (Fig. 4*E*). Finally, on the last session of the experiment, we subjected all animals to a "Competition" condition in which the landmark was incorrectly located on one of the long walls and the shape of the tank stayed rectangular (Fig. 4*F*). Here, the animals faced both boundary (based on rectangular shape) and landmark (based on incorrect landmark reference) conditions at once. The "Competition" condition informed us whether genotype differences affected the capability of mice to derive the correct spatial information for navigation independently from the main landmark.

Each group progressively reduced the latency to reach the platform across the daily sessions, which indicated that learning was not impaired in mutants compared to controls (Fig. 4*C*). In addition, the overall latency to reach the platform and the latency to first entry the zone "A," where the platform was located, during training were not statistically different among the groups (*SI Appendix*, Fig. S5 *C* and *D*). Nevertheless, the test revealed some

remarkable differences concerning the use of boundary-based versus landmark conditions in spatial navigation (51, 55, 56). In particular, both in landmark and boundary-based conditions, the wild-type animals spent significantly more time in the zone "A" (platform) compared to both heterozygous and homozygous mutants (Fig. 4 *D* and *E* and *SI Appendix*, Fig. S5*E*), suggesting that wild-type mice developed proper spatial reference information within the environment while mutants maintained a certain level of uncertainty. Moreover, in the competition condition, only wild-type mice explored more of the correct location (zone "A") (Fig. 4*F* and *SI Appendix*, Fig. S5*D*), demonstrating that the spatial information previously acquired was sufficient to permit the correct navigation in absence of the visible landmark. Indeed, the time they spent in zone "A" (platform) was significantly higher than the time spent in zone "B" (uninformative landmark) (Fig. 4*F* and *SI Appendix*, Fig. S5*E*). In contrast, heterozygotes and *Dlk1* homozygous mutant mice spent a similar time in zone A and in zone B (Fig. 4*F* and *SI Appendix*, Fig. S5*E*), confirming their uncertainty between the two types of information. All together, these results indicate that *Dlk1*-deficient animals were not able to properly use landmark or geometric information, suggesting that biallelic expression of *Dlk1* is required for spatial navigation.

Dlk1 Does Not Participate in Location Discrimination. The DG is also thought to contribute to spatial or episodic memory by functioning as a pattern separator through the formation of distinct representations of similar inputs (26, 57). This ability to form and

use memories derived from very similar stimuli that are closely presented in space and/or time depends upon the ability to pattern separate incoming information. In order to determine the potential role of *Dlk1* in spatial discrimination, we have used a spatial non-navigable task using a mouse touch screen method (17, 58) in which we analyzed pattern separation-dependent memory by testing whether mice could differentiate between two locations that were presented closely. *Dlk1* heterozygotes and *Dlk1* homozygous 2-mo-old mutant mice were tested in the touchscreen location discrimination (LD) test. Mice were assessed on two types of condition in separate sessions: the big separation (easiest) condition and small separation (hardest) condition, which heavily taxes pattern separation and which is dependent upon neurogenesis in the DG (17). Mice received 20 sessions in total, 10 of each, in pairs of each separation. In each session, mice had the opportunity to acquire a contingency—which requires them to consistently (seven out of eight consecutive trials) pick, for example, the left location and then reverse it (again, seven out of eight consecutive touches), picking, for example, the right location. Thus, the number of trials that mice require to acquire and reverse can be analyzed separately. Mice with depleted hippocampal neurogenesis show impairments discriminating similar locations with a small separation between them—that is, when there is a high load on pattern separation—but no difficulty discriminating dissimilar locations with a large separation (17). However, *Dlk1* heterozygous and homozygous mutant mice with a roughly 40% decrease in hippocampal neurogenesis had no impairment in discriminating either similar or dissimilar locations (*SI Appendix*, Fig. S6 *A* and *B*). This suggests that there may be a critical amount of neurogenesis needed to affect this behavior significantly.

Deletion of *Dlk1* in the GFAP+ Population Results in Defects in Spatial Memory Consolidation. In the adult brain, *Dlk1* is biallelically expressed in the neurogenic niches, but is also expressed in nonneurogenic regions including the ventral tegmental area, the septum, and the ventral striatum, where the gene is imprinted and expressed only from the paternal allele (33, 59, 60). Differentiated astrocytes also expressing GFAP in the SGZ niche showed very low levels of expression of *Dlk1* gene (Fig. 1*A*). Thus, in order to evaluate the regulatory function of paternal and maternal *Dlk1* specifically in the neural stem cell population from the adult SGZ, a murine conditional genetic model was generated by crossing mice carrying *loxP* sites flanking part of the *Dlk1* gene (61) with mice expressing the *Cre-recombinase* under the control of the *Gfap* promoter (62). Significant expression of Cre-recombinase in $Dlk1^{loxp/+}$-*Gfap-cre*$^{+/0}$ (with a deletion of the maternal allele and referred to as $Dlk1$-$Gfap^{MatCre}$), $Dlk1^{+/loxp}$-*Gfap-cre*$^{+/0}$ (with a deletion of the paternal allele and referred to as $Dlk1$-$Gfap^{PatCre}$), and $Dlk1^{loxp/loxp}$-*Gfap-cre*$^{+/0}$ (with a deletion of the maternal and paternal alleles and referred to as $Dlk1$-$Gfap^{Ma/PatCre}$) compared to $Dlk1^{loxp/loxp}$-*Gfap-cre*$^{0/0}$ (referred to as $Dlk1$-$Gfap^{control}$) control mice was confirmed in SGZ-derived NSCs (Fig. 5*A*). The removal of *Dlk1* messenger RNA was demonstrated specifically in neurospheres isolated from $Dlk1$-$Gfap^{MatCre}$, $Dlk1$-$Gfap^{PatCre}$, and $Dlk1$-$Gfap^{Ma/PatCre}$ deficient SGZ (Fig. 5*A*). Importantly, X-gal histochemistry in the adult brain of LACZ/ROSA26R;Gfap-cre+/0 mice (referred to as Gfap-CRE/LACZ) showed positive staining in the SGZ, of the adult Gfap-CRE/LACZ brains and colocalized with GFAP+ cells only within the SGZ (Fig. 5*B*), corroborating the specific deletion of *Dlk1* in the adult GFAP+ stem cell population.

To further investigate the role of maternal and paternal *Dlk1* in DG neurogenesis, we injected 2-mo-old $Dlk1$-$Gfap^{control}$, $Dlk1$-$Gfap^{MatCre}$, $Dlk1$-$Gfap^{PatCre}$, and $Dlk1$-$Gfap^{Mat/PatCre}$ conditional mice with the nucleotide analog BrdU 3 wk prior to killing. As previously noted, among the cells that retained BrdU, we quantified the proportion of GFAP/SOX2+ undifferentiated cells in *Dlk1* conditional mice and observed that the total number

of GFAP/SOX2+ cells was also diminished both in $Dlk1$-$Gfap^{MatCre}$ and $Dlk1$-$Gfap^{PatCre}$ conditional mice (Fig. 5 *C* and *D*). As a result, the number of DCX+ neuroblasts was significantly reduced after both maternal and paternal transmission of the mutation (Fig. 5 *C* and *D*). Consistently with nonconditional study, a more severe reduction in the GFAP/SOX2+ and newborn DCX+ cells was observed in $Dlk1$-$Gfap^{Mat/PatCre}$ conditional mice, confirming that *Dlk1* dosage regulates SGZ neurogenesis. Moreover, the number of primary neurospheres isolated from the DG was reduced in $Dlk1$-$Gfap^{MatCre}$ and $Dlk1$-$Gfap^{PatCre}$ conditional mice, which grew less efficiently than control in long-term cultures (Fig. 5 *E* and *F*). $Dlk1$-$Gfap^{Mat/PatCre}$ cultures showed a more acute growth impairment also in vitro (Fig. 5 *E* and *F*). These data demonstrate that *Dlk1* controls stem cell maintenance in the adult SGZ and that biallelic expression of the gene in the GFAP+ population regulates hippocampal neurogenesis.

We next examined the behavior of the *Dlk1* conditional mice in the EPM. The time spent and the percentage of entries in open arms, estimated during a 10-min observation period, was not affected, indicating that, similarly to wild-type and *Dlk1* heterozygous constitutive mutant mice, there was no change in overall ambulatory behavior in *Dlk1* conditional mice (Fig. 6*A*). Moreover, $Dlk1$-$Gfap^{MatCre}$ and $Dlk1$-$Gfap^{PatCre}$ conditional mice were not more anxious than wild type in agreement with our previous results in nonconditional mutants (Fig. 6*A*). To further determine whether the postnatal down-regulation of *Dlk1* in the GFAP+ population within the SGZ niche has an effect in spatial memory consolidation, we performed a Morris water maze (MWM) test in $Dlk1$-$Gfap^{control}$, $Dlk1$-$Gfap^{MatCre}$, and $Dlk1$-$Gfap^{PatCre}$ conditional mice. We used a round water maze filled up with water with a platform submerged below the surface (Fig. 6*B*) (63). A landmark was positioned close to the wall of zone A where the platform was located. To maximize the potential differences because of altered hippocampal neurogenesis between experimental groups, we used a simplified protocol in which mice entered the maze through the same quadrant (zone D) and in a straight line to the position of both the platform and the landmark (Fig. 6*B*). Each animal underwent three trials/day for only 3 d so as to acquire the task easily. After the training, we performed a probe trial with the same experimental conditions but without the platform (Fig. 6*C*). The time spent in every zone was measured (Fig. 6*C*). Consistently, during acquisition, all experimental groups progressively reduced the latency to reach the platform across the training daily sessions, which indicated similar learning in conditional mutants and controls (Fig. 6*D*). However, when the animals were tested in the probe as a first nonreinforced trial, the difference between experimental groups appeared after they failed to find the platform. Data showed that $Dlk1$-$Gfap^{control}$ mice spent significantly more time exploring zone A (where the platform was previously located) than in any other zones (Fig. 6*E*), indicating that they were able to recall a spatial association between the landmark position and the platform. In contrast, maternal and paternal *Dlk1* conditional heterozygous mice navigated randomly throughout the maze with no significant preferences between zones showing no spatial navigation-based searching strategies (Fig. 6*E*), consistent with the behavioral phenotypes observed in *Dlk1* constitutive mutant mice (Fig. 4*D*). These data confirm that biallelic expression of *Dlk1* in the neural stem cell population within the SGZ is required for spatial memory in adult mice.

Discussion

This work highlights a positive role for DLK1 in promoting NSCs self-renewal in the adult hippocampus. Both short-term and long-term (age-related) neurogenesis in the SGZ requires selective absence of imprinting of *Dlk1* and hence is sensitive to *Dlk1* dosage. We show that defective postnatal neurogenesis in constitutive *Dlk1* mutant mice is associated with an increased anxiety-related behavior in unfamiliar environments. Moreover,
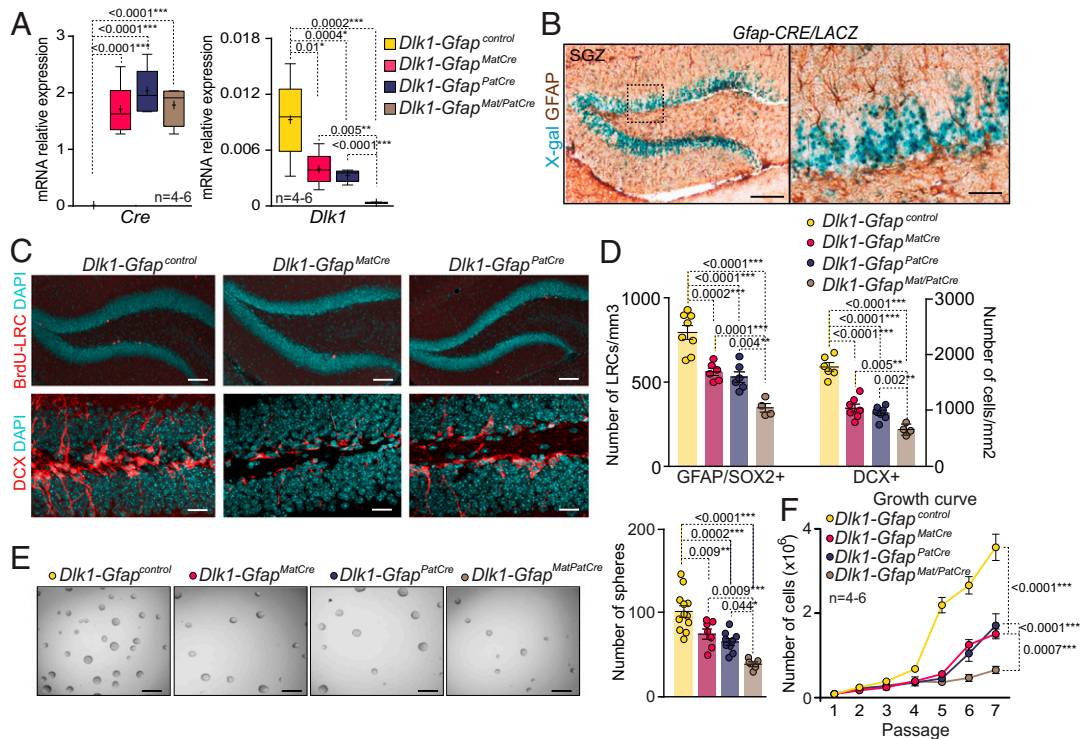
NEUROSCIENCE

Fig. 5. Specific deletion of Dlk1 in GFAP cells causes a neurogenic defect in the adult SGZ. (*A*) qPCR for *Cre-recombinase* and *Dlk1* in NSCs of *Dlk1-Gfap^control^*, *Dlk1-Gfap^MatCre^*, *Dlk1-Gfap^PatCre^*, and *Dlk1-Gfap^PatMatCre^* conditional mice. (*B*) β-galactosidase staining (blue) and immunohistochemistry for the astrocyte marker GFAP (brown) in the SGZ of Gfap-CRE/LACZ mice. Gfap-CN/LACZ samples with no Cre-recombinase were used as controls for the staining. (*C*) Immunohistochemistry for BrdU-LRC (*Upper*) and DCX (*Lower*) within the SGZ of *Dlk1-Gfap^control^*, *Dlk1-Gfap^MatCre^*, and *Dlk1-Gfap^PatCre^* mice. (*D*) Quantification of the total number of BrdU-LRCs that are double positive for GFAP and SOX2 (*Left*) and DCX positive neuroblasts in the SGZ from the different genotypes. (*E*) Representative images of the primary neurosphere cultures obtained from *Dlk1-Gfap^control^*, *Dlk1-Gfap^MatCre^*, *Dlk1-Gfap^PatCre^*, and *Dlk1-Gfap^PatMatCre^* SGZ (*Left*). Quantification of the number of primary neurospheres formed in Dlk1-deficient NSCs (*Right*). (*F*) Growth curve for *Dlk1-Gfap^control^*, *Dlk1-Gfap^MatCre^*, *Dlk1-Gfap^PatCre^*, and *Dlk1-Gfap^PatMatCre^* cultures during passages one to seven. All error bars show SEM of at least four animals per genotype. One-way ANOVA and Sidak multiple comparison tests were used. Simple linear regression analysis was applied in *F*. P values and number of samples are indicated. (Scale bar in *B* and *C*: 100 μm; high magnification images, 60 μm; in *E*: 60 μm.)

although *Dlk1*-deficient mice show normal learning, a reduction of *Dlk1* dosage triggers specific defects in performing spatial behavioral tasks. Consistently, conditional deletion of the paternal or maternal *Dlk1* alleles in the SGZ neural stem cell population confirm that biallelic expression of *Dlk1* in the GFAP+ population is necessary for hippocampal neurogenesis and for normal cognitive functions such as spatial memory consolidation.

Loss of *Dlk1* compromises the maintenance of the neural stem cell pool in the SGZ, leading to reduced neurogenesis and affecting the tripotent differentiation capacity of neural progenitors both in vivo and in vitro. In contrast to the SVZ, where DLK1 acts as an astrocyte-secreted niche factor (33), DLK1 seems to function autonomously in the DG based on the reduction of secondary neurosphere formation and proliferation capacities in SGZ progenitors isolated from *Dlk1^−/−^* mice. Accordingly, *Dlk1* is highly expressed in NSCs but nearly absent in SGZ differentiated astrocytes, in contrast to what happens in the adult SVZ (33). Deletion of *Dlk1* also causes a reduction in the number of radial NSCs and nonradial progenitors in the DG in vivo that results in a decrease in the number of DCX+ immature neurons and NeuN+ mature neurons located in the GCL. It is still not known if DLK1 is required in the SGZ to maintain quiescence at early postnatal phases as happens in the SVZ (33). Thus, these findings raise the question of how DLK1 affects adult neurogenesis in the different neurogenic niches. Whereas *Dlk1* deletion may decrease hippocampal neurogenesis simply through the repression of NSC proliferation, it is also possible that DLK1 regulates the cell cycle of populations other

than radial NSCs in the DG. However, we did not observe a significant change in the number of proliferating TBR2+ progenitors or DCX+ neuroblasts after *Dlk1* deletion; hence, the cell cycle of neural progenitors does not appear to be a major target of DLK1 in the regulation of hippocampal neurogenesis. It has been previously described that continuous depletion of the neural stem cell pool, as a consequence of their division, may contribute to the age-related decrease in hippocampal neurogenesis (49). Our data also reveal a role of DLK1 in the regulation of NSC maintenance in the long-term (age-related) modulation of neurogenesis. This is based on the observation that although deletion of *Dlk1* initially resulted in a moderate decrease of the proportion of stem cells in the SGZ of the adult hippocampus, it later led to excessive reduction in the NSC pool and impaired neurogenesis. This is consistent with the classical view of stem cell exhaustion, where cells achieve the limit of their self-renewal capacity (64), a process that seems to be accelerated in the *Dlk1* mutant SGZ. Thus, adult neurogenesis acts as a base for brain plasticity, allowing modulation of neural circuits in the hippocampus, and we show here that DLK1 plays a role in determining this rate during the entire life of the organisms.

Dlk1 is canonically expressed from the paternally inherited chromosome and belongs to the *Dlk1–Dio3* imprinted gene cluster on mouse chromosome 12. We previously confirmed *Dlk1* transcription from the paternal allele in the nonneurogenic regions of the adult brain; however, we have observed neurogenic phenotypes in both the SVZ (33) and the SGZ of heterozygotes upon maternal or paternal transmission of the mutation and in
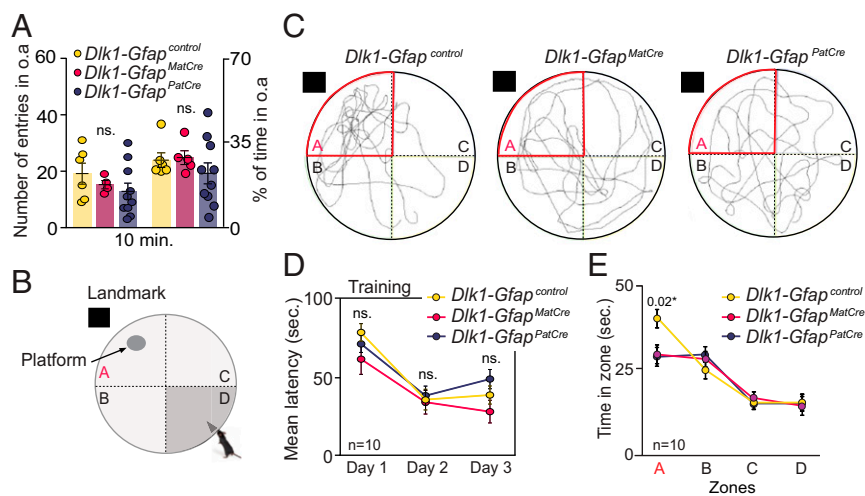
Fig. 6. Biallelic expression of *Dlk1* in the GFAP population regulates memory consolidation. (*A*) Number of entries and time spent in open arms (o.a) after a 10-min observation period in *Dlk1-Gfap*^{control}, *Dlk1-Gfap*^{MatCre}, *Dlk1-Gfap*^{PatCre}, and *Dlk1-Gfap*^{PatMatCre} conditional mice. (*B*) Schematic representation of the MWM system. The test is performed in a white circular tank with a platform and a black landmark. A, B, C, and D indicate the four zones in the tank. Mice were introduced in the water maze always from the same quadrant (zone D). (*C*) Representative images of the water maze test videos acquired for offline scoring and analyses. (*D*) Mean latency in the training phase (day 1 to day 3; *Right*) for the MWM test. (*E*) Graph representing the time spent in each zone for each group of mice. Control animals spent significantly more time in the zone "A" where the platform was located compared to *Dlk1-Gfap*^{MatCre} and *Dlk1-Gfap*^{PatCre} mice. Dashed line indicates random swim time. All error bars show SEM. One-way ANOVA and Sidak multiple comparison tests were used. Two-way ANOVA was applied in *D* and *E*. *P* values and number of samples are indicated.

Dlk1 homozygotes mutant mice. This indicates that the paternal and the maternal inherited alleles are specifically required for postnatal neurogenesis in both neurogenic niches. This supports the hypothesis that regulation of the imprinting process might be adaptable to the environmental niche in which the stem cells are acting. Indeed, we have previously shown that another imprinted gene, *Igf2*, acts differentially in the two adult neurogenic niches (65). *Igf2* is biallelically expressed in the vascular compartment, influencing the activation of the stem cell pool in the SVZ, whereas it is solely expressed from the paternal allele in the SGZ, where it acts as an autocrine factor (65). However, our data also show that other imprinted genes such as *Gtl2* or *Snrpn* maintain their imprinting state in both the SGZ, consistent with previous data in the SVZ (33). This data confirms that loss of genomic imprinting is not a generalized phenomenon in the adult brain and that the regulatory decision to imprint or not is a functionally important mechanism of transcriptional dosage control in adult neurogenesis that acts on very specific genes.

Previous research showed that deficiency of hippocampal neurogenesis impairs learning and memory (16, 66, 67). The influence of imprinted genes on behavior and memory-related processes has not been extensively studied; however, there is a growing interest in determining the relationship between genomic imprinting and complex human postnatal behaviors. For instance, the brain-specific miR-379/miR-410 gene cluster, located within the same imprinted domain as *Dlk1*, has been implicated in emotional responses and anxiety-related behavior in unfamiliar environments. In contrast, miR-379/miR-410–deficient mice showed normal learning and spatial (or contextual) memory abilities in hippocampus-dependent tasks involving neuronal plasticity (68). The authors suggested that the lack of expression of the entire microRNA cluster may be less detrimental than downregulation of miR-134 included in the cluster. They also postulated that changes in dendritic spine morphology occurring in miR-379/miR-410–deficient mice do not necessarily result in cognitive defects and that a compensatory and/or redundant pathway may operate attenuating some phenotypes (68).

Here, we examined the physiological role of *Dlk1* in adult brain functions by subjecting mice with constitutive and GFAP conditional deletion of the gene to a battery of cognitive and behavioral tests. Complete lack of *Dlk1* expression leads to increased anxiety-related phenotypes as shown by a reduced activity and number of entries in the open arms as well as the increased defecation and urination. However, *Dlk1* maternal or paternal heterozygous mice show no indication of anxiety. Importantly, adult *Dlk1* mutant mice with deficiency in adult neurogenesis show selective defects in remembering spatial information from reduced landmark conditions. In the spatial navigation test, *Dlk1*$^{mat/l+}$, *Dlk1*$^{+/pat}$, and *Dlk1*$^{-/-}$ exhibited an inferior performance when trying to localize the platform in the absence of the main landmark, while wild-type mice succeeded in all conditions. This suggests that wild-type mice can perform in spatial navigation even in the absence of the main landmark information, for example, relying on boundary information and/or other subtle environmental information. However, *Dlk1* mutation affects spatial learning retrieval. In our study, we can conclude that the overall learning acquisition process is not compromised in *Dlk1*-deficient mice, but their performance during memory tests is diminished. In accordance, mice with a specific deletion of *Dlk1* alleles in the GFAP+ stem cell population failed to find the platform after training in a MWM test and navigated randomly throughout the maze, suggesting that *Dlk1* deletion in the stem cell population has a functional effect in the hippocampus ability to consolidate spatial learning. It is worth noting that given that *Dlk1* is expressed in NSCs but nearly absent in terminally differentiated astrocytes in the SGZ, the defects found in *Dlk1* deficient mice are unlikely due to alterations of this gene in the astrocytic population. Interestingly, *Dlk1* mutants did not differ from wild types in the pattern separation task with the touch screen (17, 58), suggesting that the level of neurogenesis decrease might play a role in this more difficult task.

In the adult brain, *Dlk1* is also expressed in nonneurogenic regions including the ventral tegmental area, the septum, and the ventral striatum, where the gene is imprinted and expressed only from the paternal allele (33, 59, 60). Our data indicate that *Dlk1* mutation of the canonically nonexpressed maternal allele also causes defects in the proportion of newborn neurons incorporating to the SGZ. These findings have the potential to contribute new

insights into understanding the function of imprinted genes and the evolution of dosage control by selective absence of imprinting in particular stem cell developmental contexts. Together, these findings suggest that genomic imprinting can be used as a sophisticated mechanism of gene dosage control and raises questions about how intrinsic environmental cues modulate the adaptability and flexibility of this epigenetically regulated process. Further studies are needed to determine the role of imprinted genes and the epigenetic mechanisms underlying imprinting dynamics in the adult neurogenic niches.

Methods

Animals and In Vivo Manipulations. The generation and genotyping of *Dlk1* mutant and transgenic mice have been described previously (33, 48, 69). To generate the *Dlk1* knockout mice, a neomycin resistance cassette was used to replace 3.8 kbp of the endogenous allele, including the promoter and first three exons of *Dlk1* (33, 69). The generation of transgenic mice was done using bacterial artificial chromosomes (BACs). *Dlk1* BAC transgene contains 49.5 kb of sequence upstream of *Dlk1* and ends ~18 kb downstream of the *Dlk1* transcriptional start site (48). *Dlk1* conditional mice were generated by crossing mice carrying *loxP* sites flanking part of the *Dlk1* gene (61) with mice expressing the *Cre-recombinase* under the control of the *Gfap* promoter (62). Experiments were done with mice on a C57BL/6 genetic background and their corresponding wild-type littermates. Housing of mice and all experiments were carried out in accordance with the UK Animals (Scientific Procedures) Act 1986 and with Spanish Royal Decree 1386/2018 guidelines, under appropriate Home Office personal and project licenses.

Immunohistochemistry and BrdU Administration. After 2-mo-old mice were deeply anesthetized, they were perfused transcardially with 4% paraformaldehyde (PFA) in phosphate-buffered saline (PBS). Fixed brains were sectioned with a vibratome (Leica VT1000) at 30 μm. Mice were injected intraperitoneally with 50 mg of BrdU per kg of body weight every 2 h for 12 consecutive hours (seven injections in total) (14, 33). Mice were killed 21 d (LRC) after the last injection. For BrdU detection, sections were incubated in 2N HCl for 20 min at 37 °C, neutralized in 0.1 M sodium borate (pH 8.5), blocked in 10% fetal bovine serum (FBS) and 0.1% Triton X-100 in phosphate buffer for 1 h, and incubated overnight in primary antibodies (*SI Appendix*, Table S1a) in the same blocking buffer. Immunofluorescent detections were performed with secondary antibodies (*SI Appendix*, Table S1b). DAPI (1 μg/mL, 5 min; Molecular Probes) was used for counterstaining. Samples were analyzed with Olympus FV10 confocal microscopes. Labeled cells were counted in every 10th 30-μm section through the entire rostrocaudal length of the DG (−0.92 mm to −3.90 mm from bregma). To count GFAP+ radial cells, we used association of the cell body with a DAPI+ nucleus and a single radial process extending through the granule layer.

Cell Cultures and Cell Cycle Analysis. SGZ-derived neurosphere cultures were obtained by dissecting out DG and digestion in 0.025% trypsin and 0.265 mM ethylenediaminetetraacetic acid (Invitrogen) as previously described (13). Briefly, a single-cell suspension was obtained by gentle trituration and diluted in serum-free medium composed of Dulbecco's Modified Eagle Medium/F12 with 1% B27 supplement, 10 ng/mL EGF (Invitrogen), and 5 ng/mL bFGF (Sigma). Neurospheres were allowed to develop for 6 d in a 95% air/5% CO$_2$ humidified atmosphere at 37 °C. For secondary neurosphere assays, cells were treated with Accutase (0.5mM; Sigma) for 10 min, mechanically dissociated to a single-cell suspension and replated in growth medium containing EGF and bFGF, and supplemented or not with recombinant DLK1 (mouse) fused to Fc (human; 2 to 100 ng/mL; Enzo Life Sciences, Inc.). For culture expansion, cells were plated at high density (10 cell/μL) and maintained for several passages. To generate the accumulated cell growth curves, the ratio of cell production at each subculturing step was multiplied by the number of cells at the previous point of the curve (70). This procedure was repeated for each passage as previously described (70). Multipotency capacity was analyzed by seeding individual neurospheres of similar sizes at passage two and three in Matrigel-coated 96-well plates for 7 d in vitro (with 2% FBS, vol/vol), before fixation in 4% PFA. No fewer than 50 clones were analyzed for each condition, and the experiment was conducted as previously described (33). The distribution of unipotent clones (astrocytes, GFAP+), bipotent clones (GFAP+ astrocytes and βIII-tubulin+ neurons), and tripotent clones (GFAP+ astrocytes, βIII-tubulin+ neurons, and O4+ oligodendrocytes) was determined. To quantify the viability of cultures, the MTS Cell Proliferation Colorimetric kit (Abcam) was used. Cells were seeded at 10,000 cells/cm^2 for 2 d in growth medium. Metabolically active cells generate a colored formazan product that was quantified measuring the absorbance at 490 nm. For cell cycle analysis, 5×10^5 dissociated cells were recovered and fixed in –20 °C-cold ethanol for 30 min. Cells were then washed three times in PBS, followed by incubation with 20 μg/mL Hoechst 33342 and 0.3 mg/mL RNase at 37 °C for 30 min before analysis on an EPICS XL flow cytometer (Coulter) using CellQuest software (Becton Dickinson).

RNA Isolation and Expression Analysis. RNAs were extracted with RNeasy MicroKit (Qiagen), and 1 μg of RNA was reverse transcribed into complementary DNA (cDNA) using random primers and SuperScript II RT Reverse Transcriptase (Invitrogen) in the presence of first strand buffer (50 mM Tris HCl, 75 mM KCl, and 3 mM MgCl$_2$), 5 mM dithiothreitol, and 0.25 mM each deoxynucleotide triphosphate (Amersham) for 2 h at 42 °C. Thermocycling was performed in a final volume of 20 μL, containing 2 μL cDNA sample (diluted 1:20), and the reverse transcribed RNA was amplified by PCR with appropriate TaqMan probes (*SI Appendix*, Table S1c) as previously described (70). qPCR was used to measure gene expression levels normalized to *Gapdh*. qPCR reactions were performed in a StepOnePlus cycler with TaqMan Fast Advanced Master Mix (Applied Biosystems) (70). SYBR green thermocycling was performed in a final volume of 10 μL, containing 1 μL cDNA sample (diluted 1:20), 0.2 μM each primer (*SI Appendix*, Table S1d), and SYBR Premix Ex Taq (Takara) according to the manufacturer instructions. A standard curve made up of doubling dilutions of pooled cDNA from the samples assessed was run on each plate, and quantification was performed relative to the standard curve. For the study of *Dlk1* isoforms, Dlk1AB-F and Dlk1AB-R (*SI Appendix*, Table S1d) primers were used to amplify the secreted isoforms A and B. To amplify all the isoforms primers, Dlk1All-F and Dlk1All-R were used (*SI Appendix*, Table S1d).

Imprinting Assay. A *Dlk1* imprinting assay to analyze parental allele-specific gene expression was based on PCR amplification followed by direct sequencing as previously described (33). To determine the imprinting status of *Dlk1* and *Gtl2* in the hippocampus and SGZ-derived NSCs, we used the reciprocal F1 hybrid offspring of *Mus musculus domesticus* (strain C57BL/6, abbreviated BL6) and *Mus musculus castaneus* (strain CAST/EiJ, abbreviated Cast) subspecies in which an SNP was identified between the two subspecies within these genes. PCR reactions were purified with the QiAquick kit (Qiagen) before sequencing. The sequences of murine *Dlk1*, *Gtl2*, and *Snrpn* were obtained from GenBank (accession numbers: NM010052 for *Dlk1*, Y13832 for *Gtl2*, and NM001082961.2 for *Snrpn*). The *Dlk1* polymorphism, located at nucleotide 721 of exon 5, is a "T" in BL6 mice and a "C" in Cast mice. The *Dlk1* imprinting assay used primers Dlk1-F and Dlk1-R (*SI Appendix*, Table S1d) to amplify a fragment between exons 4 and 5, with the thermal cycler conditions as 94 °C for 1 min, 60 °C for 1 min, 72 °C for 1 min, and 30 cycles. The primer Dlk1seq was used for direct reverse PCR fragment sequencing. The *Gtl2* polymorphism, located at nucleotide 26 of exon 8, is a "C" in BL6 mice and a "T" in Cast mice. The *Gtl2* imprinting assay used primers Gtl2-F and Gtl2-R (*SI Appendix*, Table S1d) to amplify a fragment between exons 6 and 8, with the thermal cycler conditions as 94 °C for 1 min, 59 °C for 1 min, 72 °C for 1 min, and 33 cycles. Primer Gtl2-R was used for direct sequencing. Genomic DNA sequence traces from BL6 and Cast SVZs were used to identify strain-specific polymorphisms (*SI Appendix*, Fig. S1B). The *Snrpn* polymorphism, located at nucleotide 1270 of exon 10, is a "C" in BL6 mice and a "T" in Cast mice. The *Snrpn* imprinting assay used primers Snrpn-F and Snrpn-R (*SI Appendix*, Table S1d) to amplify a fragment between exons X and X, with the thermal cycler conditions as 94 °C for 1 min, 61 °C for 1 min, 72 °C for 1 min, and 32 cycles.

Behavioral tests.

Geometry test. We used a white rectangular tank (126 × 66 cm, 50 cm high) convertible into a square arena (66 × 66 cm, 50 cm high) as described (54). The tank was filled with ~9 cm of water mixed with nontoxic white paint to ensure the nonvisibility of a platform. The platform was maintained just below the level of the water and kept during the training phase of the test. Each trial started when the animal was introduced to the tank and lasted until the mouse reached the platform or after 1 min. Water represented a negative condition, and all animals explored the arena to find the platform. Before each trial, all animals were disoriented by removing them from their home cage and transported into the testing room inside a curtained cage from an adjacent room. Then, the experimenter released them into the center of the maze. The training was spread across 3 consecutive days with daily sessions of three trials. After training, we subjected all animals to a series of probe trials in which the platform was removed, and the spatial navigation of the animals was monitored and analyzed according to specific environmental conditions. Each post-training daily session started with a

probe trial followed by two training trials. These latter training trials were used to avoid extinction of the memory for the platform. The surrounding space along the apparatus was enclosed by white panels to eliminate extramaze cues, stressing the relevance of the geometric and/or landmark information. Within the tank, a black landmark (21 × 50 cm) was positioned on the short wall above the platform and stayed there for the whole training (Fig. 4C). At the end of each trial, the animals were positioned on a heating pad in order to keep them warm. Videos were acquired by a camera mounted above the tank and the ANY-maze video tracking system was used for offline scoring and analyses. For the "landmark" condition, the tank was converted into a square arena with the landmark located on the same wall as in the training condition. For the "geometry" condition, the tank was maintained in its rectangular shape with no landmark. Although we removed the main visible landmark, we could not exclude that animals were able to use subtle references within the experimental setting. The order of presentation of the two probe conditions was counterbalanced across subjects for each group. On the last session of the experiment, we subjected all animals to a "competition" condition in which the landmark was located on one of the long walls and the shape of the tank stayed rectangular. Here, the animals faced both geometric (because of the rectangular shape) and landmark (because of the landmark reference) conditions at once, where the landmark was placed in an incorrect location.

Spatial discrimination test: Mouse touch screen. This test was performed in a similar manner to previously described (17, 58). Briefly, the testing apparatus was the in-house style of operant chambers and consisted of a sound-attenuating box containing a standard modular testing chamber fitted with an infrared touch screen, a pellet receptacle with light illumination and head entry detectors, a pellet dispenser, a house light, and a tone generator (71). During the LD training, the touchscreen had response windows or locations in which white square stimuli could be presented on the screen (*SI Appendix*, Fig. S6A). Prior to LD training, mice were habituated to the apparatus, and then in a Pavlovian learning stage, they learned to associate a pellet delivery reward with the offset of a single white square stimulus on the screen, the sound of the tone, and the onset of the magazine light. Next, mice learned to nose poke to the stimulus on the screen during each of the 30 trials per session in order to obtain a reward, and then the requirement to initiate trials by nose poking into the illuminated magazine was introduced. In the final training stage, a punishment was introduced for touching one of the empty (plain black) locations instead of the correct location with the white stimulus, therefore introducing a cue signaling incorrect responses: a 10 s "time out" (stimulus disappeared, houselights off, no pellet). Following either type of response, the next trial was presented after a 10 s intertrial interval. This final stage was considered complete when at least 76% of the 30 trials were correct on two consecutive sessions, with the final session taking less than 30 min. The LD training sessions comprised 60 trials in up to 60 min (except the first two sessions, which comprised only 30 trials). On each trial, two plain white stimuli were presented in locations two and five (with two gaps between). One of these locations was initially correct and rewarded, while the other was punished. Mice "acquired" the discrimination first in each session when they achieved seven out of eight consecutive trials correct, and then the reward contingency was reversed. If mice reached the seven out of eight consecutive trials correct criterion again, they were said to have achieved "reversal" of the discrimination. The criterion for completion of this LD training was achieving an acquisition and at least one reversal on at least three out of four consecutive sessions. In the 5 d before probe testing began, all mice received five consecutive reminder sessions. Finally, mice received LD probe sessions with two different separations: the small separation used locations three and four, while the big separation used locations one and six (*SI Appendix*, Fig. S6A). The separation received first and initial correct side (left/right) were counterbalanced across genotype and performance on the LD reminder sessions. Otherwise, the probe sessions were identical to LD training sessions, except that the number of reversals per session was limited to one acquisition and one reversal, and mice were allowed unlimited trials in a 60-min session. All mice completed at least 60 trials in sessions which were not terminated due to reaching reversal criterion. Mice received double alternating sessions of each separation (i.e., big, big, small, small, etc.). On the first session of each pair of probes, the correct side was that assigned during the initial counterbalancing. On the second day, the correct side was that which was correct at the end of the

previous session. Mice received 20 sessions of probes, that is, five pairs of each separation.

EPM. The maze consists of four arms arranged in a cross configuration and elevated from the floor. The two opposing "closed" arms have walls (but are open at the top), while the "open" arms do not. Anxious mice would be expected to avoid the open arms. The mouse is placed into the center of the maze, facing an "open" arm, and its movements in the maze are recorded during a 10-min session. At the end of the session, the mouse is removed and the number of urine patches and fecal boli are recorded by an experimenter blind to genotype. Several parameters are measured, such as the percentage of arm entries into open arms, which is the number of entries into open arms × 100 divided by entries into open arms plus entries into closed arms; the percentage of arm time (seconds) spent in the open arms, which is the open arm time × 100 divided by open arm time plus closed arm time; and the percentage of arm activity (distance in cm) occurring in open arms, which is the distance in open arms × 100 divided by distance in open arms plus distance in closed arms. In addition, the total distance (centimeters) traveled in all zones, including the center of the maze, provides a measure of overall activity (which is potentially confounding).

MWM. The maze consists of a pale blue, plastic, round water maze very similar in measures to the original MWM (63) (120 cm diameter, 25 cm height). The maze was filled up with ~20 cm high of water mixed with nontoxic white colorant in order to camouflage a 10-cm diameter round platform located in the left superior quadrant (referred as Zone A in Fig. 6). The platform was submerged 1 cm below the surface. Water was maintained at 20 °C and it was cleaned every day. The testing room was clear of any external clues except for a 60 cm high landmark positioned close to the wall of Zone A. The landmark and platform were maintained exactly in the same position every experimental day. Every trial and test was recorded with a webcam hung 2 m over the water maze. The SMART video tracking system (Panlab) was used for offline evaluation and analyses. Mice were nicely introduced (not dropped) in the water maze, always from the same quadrant (Zone D) and in a straight line to the position of both the platform and the landmark (Fig. 6B). Experimental animals were trained with three trials per day during 3 consecutive days. The trial's time was stopped when the mouse found the target or was limited to 100 (first trial) or 90 (second and third trials and experimental test) s to avoid mice exhaustion. During the first two trials, mice that did not find the target were gently guided to it, as recommended (72). After 3 d of training, we performed the memory test with the same experimental conditions but no present target or platform. The time spent in every zone was evaluated.

Statistical analysis. All statistical tests were performed using SPSS software (version 26.0.0 for windows; SPSS, Inc.). The significance of the differences between groups was evaluated using the most appropriate test for each case: *t* tests, one or two-way ANOVA (using Tukey's, Dunnett, or Sidak post hoc tests), Kruskal–Wallis tests (using Dunn post hoc test), or linear regression. When comparisons were performed with relative values (percentages), normalization of data were done using a square root transformation. Data were always presented as the mean ± SEM. Number of experiments (*n*) performed with independent animals/cultures are indicated. Box and whisker plots show the median (horizontal line in box), mean (+), and minimum and maximum values. Values of $P < 0.05$ were considered statistically significant.

1. D. A. Lim, A. Alvarez-Buylla, The adult ventricular-subventricular zone (V-SVZ) and olfactory bulb (OB) neurogenesis. *Cold Spring Harb. Perspect. Biol.* **8**, a018820 (2016).

2. F. H. Gage, G. Kempermann, T. D. Palmer, D. A. Peterson, J. Ray, Multipotent progenitor cells in the adult dentate gyrus. *J. Neurobiol.* **36**, 249–266 (1998).

3. J. T. Gonçalves, S. T. Schafer, F. H. Gage, Adult neurogenesis in the Hippocampus: From stem cells to behavior. *Cell* **167**, 897–914 (2016).

4. F. Doetsch, I. Caillé, D. A. Lim, J. M. García-Verdugo, A. Alvarez-Buylla, Subventricular zone astrocytes are neural stem cells in the adult mammalian brain. *Cell* **97**, 703–716 (1999).

NEUROSCIENCE

5. A. L. Ferri *et al.*, Sox2 deficiency causes neurodegeneration and impaired neurogenesis in the adult mouse brain. *Development* **131**, 3805–3819 (2004).

6. H. Suh *et al.*, In vivo fate analysis reveals the multipotent and self-renewal capacities of Sox2+ neural stem cells in the adult hippocampus. *Cell Stem Cell* **1**, 515–528 (2007).

7. C. Zhao, W. Deng, F. H. Gage, Mechanisms and functional implications of adult neurogenesis. *Cell* **132**, 645–660 (2008).

8. J. B. Aimone *et al.*, Regulation and function of adult neurogenesis: From genes to cognition. *Physiol. Rev.* **94**, 991–1026 (2014).

9. S. Lugert *et al.*, Quiescent and active hippocampal neural stem cells with distinct morphologies respond selectively to physiological and pathological stimuli and aging. *Cell Stem Cell* **6**, 445–456 (2010).

10. G. L. Ming, H. Song, Adult neurogenesis in the mammalian brain: Significant answers and significant questions. *Neuron* **70**, 687–702 (2011).

11. Z. Nicola, K. Fabel, G. Kempermann, Development of the adult neurogenic niche in the hippocampus of mice. *Front. Neuroanat.* **9**, 53 (2015).

12. B. A. Reynolds, S. Weiss, Generation of neurons and astrocytes from isolated cells of the adult mammalian central nervous system. *Science* **255**, 1707–1710 (1992).

13. T. L. Walker, G. Kempermann, One mouse, two cultures: Isolation and culture of adult neural stem cells from the two neurogenic zones of individual mice. *J. Vis. Exp.*, e51225 (2014).

14. S. R. Ferron *et al.*, A combined ex/in vivo assay to detect effects of exogenously added factors in neural stem cells. *Nat. Protoc.* **2**, 849–859 (2007).

15. E. A. Pastrana, S. Estronza, I. J. Sosa, Vagus nerve stimulation for intractable seizures in children: The University of Puerto Rico experience. *P. R. Health Sci. J.* **30**, 128–131 (2011).

16. G. Berdugo-Vega *et al.*, Increasing neurogenesis refines hippocampal activity rejuvenating navigational learning strategies and contextual memory throughout life. *Nat. Commun.* **11**, 135 (2020).

17. C. D. Clelland *et al.*, A functional role for adult hippocampal neurogenesis in spatial pattern separation. *Science* **325**, 210–213 (2009).

18. J. S. Snyder, N. S. Hong, R. J. McDonald, J. M. Wojtowicz, A role for adult neurogenesis in spatial long-term memory. *Neuroscience* **130**, 843–852 (2005).

19. J. S. Snyder, A. Soumier, M. Brewer, J. Pickel, H. A. Cameron, Adult hippocampal neurogenesis buffers stress responses and depressive behaviour. *Nature* **476**, 458–461 (2011).

20. G. Kempermann, H. Song, F. H. Gage, Neurogenesis in the adult Hippocampus. *Cold Spring Harb. Perspect. Biol.* **7**, a018812 (2015).

21. H. G. Kuhn, T. Toda, F. H. Gage, Adult hippocampal neurogenesis: A coming-of-age story. *J. Neurosci.* **38**, 10401–10410 (2018).

22. T. Nakashiba *et al.*, Young dentate granule cells mediate pattern separation, whereas old granule cells facilitate pattern completion. *Cell* **149**, 188–201 (2012).

23. A. Sahay *et al.*, Increasing adult hippocampal neurogenesis is sufficient to improve pattern separation. *Nature* **472**, 466–470 (2011).

24. A. Sahay, D. A. Wilson, R. Hen, Pattern separation: A common function for new neurons in hippocampus and olfactory bulb. *Neuron* **70**, 582–588 (2011).

25. K. Y. Liu, R. L. Gould, M. C. Coulson, E. V. Ward, R. J. Howard, Tests of pattern separation and pattern completion in humans-A systematic review. *Hippocampus* **26**, 705–717 (2016).

26. P. E. Gilbert, R. P. Kesner, I. Lee, Dissociating hippocampal subregions: Double dissociation between dentate gyrus and CA1. *Hippocampus* **11**, 626–636 (2001).

27. M. R. Hunsaker, J. S. Rosenberg, R. P. Kesner, The role of the dentate gyrus, CA3a,b, and CA3c for detecting spatial and environmental novelty. *Hippocampus* **18**, 1064–1073 (2008).

28. V. Tucci, A. R. Isles, G. Kelsey, A. C. Ferguson-Smith; Erice Imprinting Group, Genomic imprinting and physiological processes in mammals. *Cell* **176**, 952–965 (2019).

29. A. Lozano-Ureña, R. Montalbán-Loro, A. C. Ferguson-Smith, S. R. Ferrón, Genomic imprinting and the regulation of postnatal neurogenesis. *Brain Plast.* **3**, 89–98 (2017).

30. J. D. Perez, N. D. Rubinstein, C. Dulac, New perspectives on genomic imprinting, an essential and multifaceted mode of epigenetic control in the developing and adult brain. *Annu. Rev. Neurosci.* **39**, 347–384 (2016).

31. B. M. Abdallah *et al.*, Regulation of human skeletal stem cells differentiation by Dlk1/Pref-1. *J. Bone Miner. Res.* **19**, 841–852 (2004).

32. M. Charalambous *et al.*, Imprinted gene dosage is critical for the transition to independent life. *Cell Metab.* **15**, 209–221 (2012).

33. S. R. Ferrón *et al.*, Postnatal loss of Dlk1 imprinting in stem cells and niche astrocytes regulates neurogenesis. *Nature* **475**, 381–385 (2011).

34. B. Mirshekar-Syahkal *et al.*, Dlk1 is a negative regulator of emerging hematopoietic stem and progenitor cells. *Haematologica* **98**, 163–171 (2013).

35. J. V. Schmidt, P. G. Matteson, B. K. Jones, X. J. Guan, S. M. Tilghman, The Dlk1 and Gtl2 genes are linked and reciprocally imprinted. *Genes Dev.* **14**, 1997–2002 (2000).

36. S. Takada *et al.*, Delta-like and gtl2 are reciprocally expressed, differentially methylated linked imprinted genes on mouse chromosome 12. *Curr. Biol.* **10**, 1135–1138 (2000).

37. K. A. Chase, J. E. Mallari, Y. Tan, L. Sittig, Behavioral effects of neuronal, parent-specific Commd1 knockout in mice. *Neuroscience* **434**, 1–7 (2020).

38. A. S. Garfield *et al.*, Distinct physiological and behavioural functions for parental alleles of imprinted Grb10. *Nature* **469**, 534–538 (2011).

39. G. Lassi *et al.*, Loss of Gnas imprinting differentially affects REM/NREM sleep and cognition in mice. *PLoS Genet.* **8**, e1002706 (2012).

40. G. Lassi *et al.*, Working-for-Food behaviors: A preclinical study in prader-willi mutant mice. *Genetics* **204**, 1129–1138 (2016).

41. L. S. Wilkinson, W. Davies, A. R. Isles, Genomic imprinting effects on brain development and function. *Nat. Rev. Neurosci.* **8**, 832–843 (2007).

42. R. d'Isa *et al.*, Mice lacking Ras-GRF1 show contextual fear conditioning but not spatial memory impairments: Convergent evidence from two independently generated mouse mutant lines. *Front. Behav. Neurosci.* **5**, 78 (2011).

43. K. P. Giese *et al.*, Hippocampus-dependent learning and memory is impaired in mice lacking the Ras-guanine-nucleotide releasing factor 1 (Ras-GRF1). *Neuropharmacology* **41**, 791–800 (2001).

44. J. Sun *et al.*, UBE3A regulates synaptic plasticity and learning and memory by controlling SK2 channel endocytosis. *Cell Rep.* **12**, 449–461 (2015).

45. D. Y. Chen *et al.*, A critical role for IGF-II in memory consolidation and enhancement. *Nature* **469**, 491–497 (2011).

46. M. A. Bonaguidi *et al.*, In vivo clonal analysis reveals self-renewing and multipotent adult neural stem cell characteristics. *Cell* **145**, 1142–1155 (2011).

47. S. J. Bray, S. Takada, E. Harrison, S. C. Shen, A. C. Ferguson-Smith, The atypical mammalian ligand Delta-like homologue 1 (Dlk1) can regulate Notch signalling in Drosophila. *BMC Dev. Biol.* **8**, 11 (2008).

48. S. T. da Rocha *et al.*, Gene dosage effects of the imprinted delta-like homologue 1 (dlk1/pref1) in development: Implications for the evolution of imprinting. *PLoS Genet.* **5**, e1000392 (2009).

49. J. M. Encinas *et al.*, Division-coupled astrocytic differentiation and age-related depletion of neural stem cells in the adult hippocampus. *Cell Stem Cell* **8**, 566–579 (2011).

50. A. Bahi, Y. S. Mineur, M. R. Picciotto, Blockade of protein phosphatase 2B activity in the amygdala increases anxiety- and depression-like behaviors in mice. *Biol. Psychiatry* **66**, 1139–1146 (2009).

51. G. Vallortigara, V. A. Sovrano, C. Chiandetti, Doing socrates experiment right: Controlled rearing studies of geometrical knowledge in animals. *Curr. Opin. Neurobiol.* **19**, 20–26 (2009).

52. S. A. Lee, V. Tucci, V. A. Sovrano, G. Vallortigara, Working memory and reference memory tests of spatial navigation in mice (Mus musculus). *J. Comp. Psychol.* **129**, 189–197 (2015).

53. C. F. Doeller, N. Burgess, Distinct error-correcting and incidental learning of location relative to landmarks and boundaries. *Proc. Natl. Acad. Sci. U.S.A.* **105**, 5909–5914 (2008).

54. L. Fellini, M. Schachner, F. Morellini, Adult but not aged C57BL/6 male mice are capable of using geometry for orientation. *Learn. Mem.* **13**, 473–481 (2006).

55. C. Chiandetti, G. Vallortigara, Spatial reorientation in large and small enclosures: Comparative and developmental perspectives. *Cogn. Process.* **9**, 229–238 (2008).

56. L. Tommasi, C. Chiandetti, T. Pecchia, V. A. Sovrano, G. Vallortigara, From natural geometry to spatial cognition. *Neurosci. Biobehav. Rev.* **36**, 799–824 (2012).

57. J. K. Leutgeb, S. Leutgeb, M. B. Moser, E. I. Moser, Pattern separation in the dentate gyrus and CA3 of the hippocampus. *Science* **315**, 961–966 (2007).

58. C. A. Oomen *et al.*, The touchscreen operant platform for testing working memory and pattern separation in rats and mice. *Nat. Protoc.* **8**, 2006–2021 (2013).

59. M. Bauer *et al.*, Delta-like 1 participates in the specification of ventral midbrain progenitor derived dopaminergic neurons. *J. Neurochem.* **104**, 1101–1115 (2008).

60. N. S. Christophersen *et al.*, Midbrain expression of Delta-like 1 homologue is regulated by GDNF and is associated with dopaminergic differentiation. *Exp. Neurol.* **204**, 791–801 (2007).

61. O. K. Appelbe, A. Yevtodiyenko, H. Muniz-Talavera, J. V. Schmidt, Conditional deletions refine the embryonic requirement for Dlk1. *Mech. Dev.* **130**, 143–159 (2013).

62. A. D. Garcia, N. B. Doan, T. Imura, T. G. Bush, M. V. Sofroniew, GFAP-expressing progenitors are the principal source of constitutive neurogenesis in adult mouse forebrain. *Nat. Neurosci.* **7**, 1233–1241 (2004).

63. W. A. MacDonald, M. R. Mann, Epigenetic regulation of genomic imprinting from germ line to preimplantation. *Mol. Reprod. Dev.* **81**, 126–140 (2014).

64. T. E. Kippin, D. J. Martens, D. van der Kooy, p21 loss compromises the relative quiescence of forebrain stem cell proliferation leading to exhaustion of their proliferation capacity. *Genes Dev.* **19**, 756–767 (2005).

65. S. R. Ferrón *et al.*, Differential genomic imprinting regulates paracrine and autocrine roles of IGF2 in mouse adult neurogenesis. *Nat. Commun.* **6**, 8265 (2015).

66. W. Deng, J. B. Aimone, F. H. Gage, New neurons and new memories: How does adult hippocampal neurogenesis affect learning and memory? *Nat. Rev. Neurosci.* **11**, 339–350 (2010).

67. C. L. Zhang, Y. Zou, W. He, F. H. Gage, R. M. Evans, A role for adult TLX-positive neural stem cells in learning and behaviour. *Nature* **451**, 1004–1007 (2008).

68. V. Marty *et al.*, Deletion of the miR-379/miR-410 gene cluster at the imprinted Dlk1-Dio3 locus enhances anxiety-related behaviour. *Hum. Mol. Genet.* **25**, 728–739 (2016).

69. R. Raghunandan *et al.*, Dlk1 influences differentiation and function of B lymphocytes. *Stem Cells Dev.* **17**, 495–507 (2008).

70. R. Montalbán-Loro *et al.*, TET3 prevents terminal differentiation of adult NSCs by a non-catalytic action at Snrpn. *Nat. Commun.* **10**, 1726 (2019).

71. A. E. Horner *et al.*, The touchscreen operant platform for testing learning and memory in rats and mice. *Nat. Protoc.* **8**, 1961–1984 (2013).

72. C. V. Vorhees, M. T. Williams, Morris water maze: Procedures for assessing spatial and related forms of learning and memory. *Nat. Protoc.* **1**, 848–858 (2006).